*Revista Mexicana de Astronomía y Astrofísica*, **59**, 123–135 (2023)

https://doi.org/10.22201/ia.01851101p.2023.59.01.09

# PHOTOMETRIC STUDY OF TWO CONTACT BINARY SYSTEMS AND A DETACHED LATE DWARF + M DWARF COMPONENTS

R. Michel[1], C. Barani[2], M. Martignoni[3], F. Acerbi[4], and L. Altamirano-Dévora[1,5]

*Received July 3 2022; accepted January 2 2023*

ABSTRACT

The results of our study of the eclipsing binary systems AF LMi, CzeV188 and CRTS J073333.0+302556 based on new CCD $B, V, R_C, I_C$ complete light curves, are here presented. The short periods of these systems are confirmed and revised. The light curves were modeled using the latest version of the Wilson-Devinney code and, as a result, we found that AF LMi (G3+G9) and CzeV188 (K0+K1) are W UMa-type contact binary systems belonging to the W subclass, showing a shallow degree of fill-out with components in good thermal contact. CRTS J073333.0+302556 is a detached binary system composed by a late dwarf (K8) and an M6 dwarf spectral type components. The asymmetries of the light curves were accounted for with a spot on the surface of one of the component. The absolute elements of the three objects were estimated.

RESUMEN

Se presentan los resultados de nuestro estudio de los sistemas binarios eclipsantes AF LMi, CzeV188 y CRTS J073333.0+302556 los cuales están basados en nuevas curvas de luz completas tomadas con CCD y los filtros $B, V, R_C, I_C$. Los cortos periodos de estos sistemas se confirman y actualizan. Las curvas de luz han sido modeladas con la última versión del código Wilson-Devinney y, como resultado, encontramos que AF LMi (G3+G9) y CzeV188 (K0+K1) son binarias en contacto del tipo W UMa pertenecientes a la subclase W, presentado un bajo grado de relleno y con las componetes en buen contacto térmico. CRTS J073333.0+302556 es un sistema binario separado compuesto por una enana tardía (K8) y una enana de tipo espectral M6. Las asimetrías encontradas en las curvas de luz fueron tomadas en cuenta con una mancha en la superficie de una de las componentes. Se ha hecho una estimación de los valores absolutos de los parámetros de los tres sistemas.

*Key Words:* binaries: close — stars: fundamental parameters — stars: individual: AF LMi, CzeV188, CRTS J073333.0+302556 — techniques: photometric



## 1. INTRODUCTION

Eclipsing binary systems can be divided in three groups, detached, semidetached, and contact, and are important objects for our understanding of the properties of stars, as well as stellar systems. The above sequence can be interpreted as different evolutionary stages, governed by the mass transfer of the massive component. Detached binaries (DB) that are eclipsing, exhibit Algol-type (EA type) light curves and the interactions between their components are quite weak. When one of the components of the detached binary system fills its Roche lobe, mass transfers to its companion start and a semidetached system is formed.

The continuing mass transfer produces the formation of a common envelope around the components with the consequent formation of a contact system (W UMa-type). The semidetached-contact phase is suggested by the thermal relaxation oscillation theory (TRO theory) (Lucy 1976; Flannery 1976; Robertson & Eggleton 1977; Yakut & Eggleton 2005; Li et al. 2008), which predicts that binaries

[1]Instituto de Astronomía, UNAM. Ensenada, México.
[2]Via Molinetto 35, 26845 Triulza di Codogno (LO), Italy.
[3]Stazione Astronomica Betelgeuse, Magnago, Italy.
[4]Via Zoncada 51, 26845 Codogno (LO), Italy.
[5]Universidad Autónoma de Baja California, Ensenada, México.

evolve oscillating in a cycle of contact-semidetached-contact states via mass transfer between the components. Moreover, K-type contact binaries with periods shorter than 0.3 days are important systems for explaining the period cut-off phenomenon (Liu et al. 2014). However, only few systems are well studied, especially those with periods shorter than 0.25 days. AF LMi was reported as variable star by Khruslov (2007) in his second list of new short periodic eclipsing binaries. He proposed its typology of variation as EW, as suggested by only 0.1 mag difference between the minima.

Details about the system CzeV188 were first published in the Open European Journal on Variable Stars (OEJV) nr. 185 (Skarka et al. 2017) where the typology of EW variation was proposed. The present study on this system is interesting because its orbital period is below the period cut-off and because of its K spectral type.

Finally, CRTS J073333.0+302556 was found to be a variable star with a period of 0.267498 days and amplitude of variations of 0.16 mag, in the Catalina Surveys Periodic Variable Star Catalog (Drake et al. 2014).

## 2. OBSERVATIONS

Observations were done at the San Pedro Martir Observatory (Mexico) with the 0.84-m telescope (an f/15 Ritchey-Chretien), the Mexman filter-wheel and the *Spectral Instruments 1* CCD detector (an e2v CCD42-40 chip with 13.5×13.5 $\mu^2$ pixels, gain of 1.39 $e^-$/ADU and readout noise of 3.54 $e^-$). The field of view was $7.6' \times 7.6'$ and binning 2×2 was employed during all the observations.

AF LMi was observed on February 3, 2016 for 0.7h, January 17, 2018 for 4.2h, April 20, 2018 for 2.3h, May 2, 2018 for 5.1h, and April, 15 2021 for 2.8h. Alternated exposures in filters $B$, $V$, $R_c$ and $I_c$, with exposure times of 30, 20, 15 and 15 seconds respectively, were taken in all the observing runs.

CzeV188 was observed on July 2, 2017 for 4.7h, July 4, 2017 for 0.6h, June 12, 2018 for 4.3h, and June 13, 2018 for 0.5h. Alternated exposures in filters $B$, $V$, $R_c$ and $I_c$ with exposure times of 40, 20, 15 and 15 seconds respectively, were taken in all the observing runs.

CRTS J073333.0+302556 was observed January 18, 2017 for 4.6h, January 28, 2017 for 7.1h, and February 3, 2017 for 6.1h. Alternated exposures in filters $B$, $V$ and $R_c$ with exposure times of 80, 30 and 15 seconds respectively, were taken in all the observing runs.

All the images were processed using IRAF[6] routines. Images were bias subtracted and flat field corrected before the instrumental magnitudes were computed with the standard aperture photometry method.

The field stars were also calibrated in the $UBV(RI)_c$ system with the help of Landolt's photometric standards (Landolt 2009). Based on this information we were able to choose comparison stars with colors similar to the variables (making differential extinction corrections negligible). For the case of AF LMi, star 2MASSJ10381377+3219597 ($U = 15.046, B = 15.051, V = 14.429, R = 14.054, I = 13.694$) was employed while 2MASSJ19493362+3141488 ($U = 14.041, B = 13.008, V = 11.773, R = 11.121, I = 10.545$) was used for CzeV188 and 2MASSJ07334403+3024524 ($U = 19.624, B = 18.355, V = 16.933, R = 16.079, I = 15.282$) in the case of CRTS J073333.0+302556. From our observations we determined the apparent magnitude $m_v$ in quadrature for AF LMi while for Cze V188 we calculated the $V$ magnitude using equations (23) of Fukugita et al. (1996)

All the obtained light curves are shown in Figure 6.

Any part of the data can be provided upon request.

## 3. PERIOD ANALYSIS AND NEW EPHEMERIS

The first ephemeris of AF LMi was proposed by Khruslov (2007) as:

$$Min.I(HJD) = 2451475.948 + 0^d.40660 \times E\,. \quad (1)$$

Subsequently, the system was observed by the All-Sky Automated Survey for Super Novae, (ASAS-SN) (Shappee et al. 2014; Kochanek et al. 2017), and a more precise period of 0.4065976d was obtained. From our observations we obtained one new time of minimum (ToM) by the fourth-order polynomial fit method.

One ToM was determined for each filter and finally they were conveniently averaged to adopt one ToM per epoch. Another 56 ToMs were obtained from the 1SWASP observations (Butters et al. 2010) and 8 more published in literature, were extracted from the "O-C gateway" database. The whole set of

[6]IRAF is distributed by the National Optical Observatories, operated by the Association of Universities for Research in Astronomy, Inc., under cooperative agreement with the National Science Foundation.

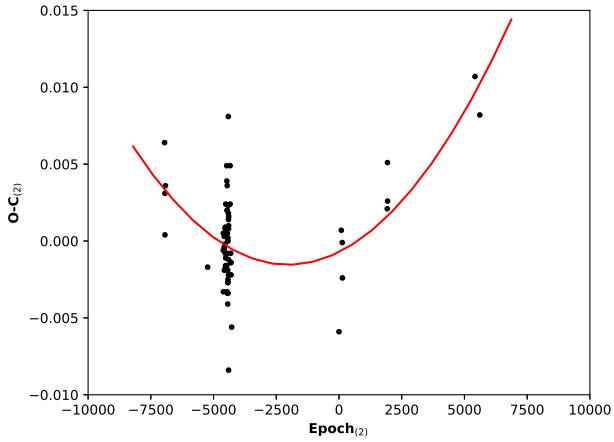


Fig. 1. O-C diagram of AF LMi related to Equation 2. The solid curve shows the second order polynomial fit to the data points. The color figure can be viewed online.

ToMs is listed in Table 1 and was used to determine new ephemeris as follows:

$$Min.I(HJD) = 2455598.8733(8) + 0^d.40659790(2) \times E + 2.016^{-10}(\pm 4.125^{-11}) \times E^2\,, \quad (2)$$

and the construction of the O-C diagram depicted in Figure 1.

The linear square fitting to the O-C data was used to obtain the new ephemeris for all the three systems.

For CzeV188, a period of 0.250295d was firstly proposed by (Skarka et al. 2017). After new observations during the ASAS-SN survey (Shappee et al. 2014; Kochanek et al. 2017), a new period of 0.2474002d was suggested. The ephemeris published in the VSX database is:[7]

$$Min.I(HJD) = 2456149.54952 + 0^d.247306 \times E\,. \quad (3)$$

Using the ToMs obtained from our observations (Table 2) of CzeV188, determined by the polynomial fit method, we can refine its ephemeris as follow:

$$Min.I(HJD) = 2456149.5494(11) + 0^d.2474007(2) \times E\,. \quad (4)$$

[7]The VSX (Variable Star IndeX) database is a web interface accessible to the public, in which one can find an exhaustive set of data for a single variable star. It is managed by the American Association of Variable Star Observers (AAVSO) and to date contains data for more than 2.2 million of variable stars.

From our observations of CRTS J073333.0+302556 we obtained 3 ToMs (Table 3), determined by the fourth-order polynomial fit method, giving a refined ephemeris of:

$$Min.I(HJD) = 2457771.8069(18) + 0^d.2674736(437) \times E\,. \quad (5)$$

## 4. MODELLING THE LIGHT CURVES

The latest version of the Wilson–Devinney (WD) code (Wilson & Devinney 1971; Wilson 1990; Wilson 1994; Wilson & van Hamme. 2016) was used and, since there are no reported spectroscopic mass-ratios of these systems, the $q$-search method was applied to find best initial values to be used during the light curve analysis.

The shape of the light curves of AF LMi and CzeV188 are clearly similar to those of W UMa systems, so we started our analysis directly in Mode 3 for overcontact binaries. Since CRTS J073333.0+302556 is a detached system, we used the appropriate Mode 2 in our calculations with no constrain on the potentials. CRTS J073333.0+302556 shows a flat primary eclipse covering approximately 0.040, 0.059 and 0.070 in phase respectively in the $B$, $V$ and $R_C$ filters.

To determine the mean surface temperature of the hotter star for AF LMi, we took the average value from the temperature indicated in different catalogues: LAMOST DR2 and DR5 catalogs (Luo et al. 2016, Luo et al. 2019), ATLAS all-sky stellar reference catalog (Tonry et al. 2018), Regression of stellar effective temperatures in GaiaDR2 (Bai et al. 2019) and CRTS Variable Sources Catalogue (Marsh et al. 2017). The average is 5700K.

For CzeV188 we used the color index $J - K = 0.524$ reported in the OEJV 185 (Skarka et al. 2017) deriving the temperature from the tables of Worthey & Lee (2011). We also used the regression of stellar effective temperatures in Gaia DR2 (Bai et al. 2019). The average temperature was found to be 5270K.

Finally, for CRTS J073333.0+302556 we used the 4027K temperature value reported by the GAIA DR2 collaboration (Gaia Collaboration 2018).

For the two contact systems, the limb-darkening parameters were interpolated with a square root law from the tables of van Hamme (1993) for $\log(g) = 4.0$ and solar abundances, while for CRTS J073333.0+302556 we used the tables of Claret & Bloemen (2011) again for $\log(g) = 4.0$ and solar abundances. A search for a solution was made

TABLE 1

TIMES OF MINIMA FOR AF LMI

| HJD | $Epoch_{(1)}$ | $O\text{-}C_{(1)}$ | $Epoch_{(2)}$ | $O\text{-}C_{(2)}$ | Error | Source |
|---|---|---|---|---|---|---|
| 2453132.4207 | -6951.5 | 0.0332 | -6951.5 | 0.0064 | 0.0002 | SWASP |
| 2453137.4998 | -6939.0 | 0.0298 | -6939.0 | 0.0031 | 0.0003 | SWASP |
| 2453138.5136 | -6936.5 | 0.0271 | -6936.5 | 0.0004 | 0.0004 | SWASP |
| 2453146.4454 | -6917.0 | 0.0302 | -6917.0 | 0.0036 | 0.0002 | SWASP |
| 2453830.5396 | -5234.5 | 0.0199 | -5234.5 | -0.0017 | 0.0004 | SWASP |
| 2454083.6474 | -4612.0 | 0.0192 | -4612.0 | -0.0006 | 0.0003 | SWASP |
| 2454084.6650 | -4609.5 | 0.0203 | -4609.5 | 0.0005 | 0.0003 | SWASP |
| 2454085.6776 | -4607.0 | 0.0164 | -4607.0 | -0.0033 | 0.0003 | SWASP |
| 2454098.6917 | -4575.0 | 0.0193 | -4575.0 | -0.0004 | 0.0002 | SWASP |
| 2454099.7088 | -4572.5 | 0.0199 | -4572.5 | 0.0003 | 0.0002 | SWASP |
| 2454100.7245 | -4570.0 | 0.0191 | -4570.0 | -0.0005 | 0.0002 | SWASP |
| 2454101.7396 | -4567.5 | 0.0177 | -4567.5 | -0.0019 | 0.0003 | SWASP |
| 2454111.7030 | -4543.0 | 0.0194 | -4543.0 | -0.0002 | 0.0002 | SWASP |
| 2454114.5485 | -4536.0 | 0.0187 | -4536.0 | -0.0008 | 0.0002 | SWASP |
| 2454114.7535 | -4535.5 | 0.0204 | -4535.5 | 0.0009 | 0.0002 | SWASP |
| 2454115.5666 | -4533.5 | 0.0203 | -4533.5 | 0.0008 | 0.0003 | SWASP |
| 2454118.6136 | -4526.0 | 0.0178 | -4526.0 | -0.0017 | 0.0002 | SWASP |
| 2454120.6467 | -4521.0 | 0.0179 | -4521.0 | -0.0016 | 0.0003 | SWASP |
| 2454122.6801 | -4516.0 | 0.0183 | -4516.0 | -0.0011 | 0.0003 | SWASP |
| 2454123.7001 | -4513.5 | 0.0218 | -4513.5 | 0.0024 | 0.0002 | SWASP |
| 2454139.5600 | -4474.5 | 0.0243 | -4474.5 | 0.0049 | 0.0002 | SWASP |
| 2454140.5699 | -4472.0 | 0.0177 | -4472.0 | -0.0016 | 0.0002 | SWASP |
| 2454141.5919 | -4469.5 | 0.0232 | -4469.5 | 0.0039 | 0.0002 | SWASP |
| 2454142.6012 | -4467.0 | 0.0160 | -4467.0 | -0.0033 | 0.0003 | SWASP |
| 2454145.6560 | -4459.5 | 0.0213 | -4459.5 | 0.0020 | 0.0002 | SWASP |
| 2454146.4692 | -4457.5 | 0.0213 | -4457.5 | 0.0020 | 0.0003 | SWASP |
| 2454147.4873 | -4455.0 | 0.0229 | -4455.0 | 0.0036 | 0.0003 | SWASP |
| 2454147.6862 | -4454.5 | 0.0185 | -4454.5 | -0.0008 | 0.0002 | SWASP |
| 2454150.5337 | -4447.5 | 0.0198 | -4447.5 | 0.0005 | 0.0002 | SWASP |
| 2454153.5792 | -4440.0 | 0.0158 | -4440.0 | -0.0034 | 0.0002 | SWASP |
| 2454154.5991 | -4437.5 | 0.0192 | -4437.5 | 0.0000 | 0.0003 | SWASP |
| 2454155.6115 | -4435.0 | 0.0151 | -4435.0 | -0.0041 | 0.0003 | SWASP |
| 2454156.4269 | -4433.0 | 0.0173 | -4433.0 | -0.0019 | 0.0001 | SWASP |
| 2454156.6321 | -4432.5 | 0.0192 | -4432.5 | 0.0000 | 0.0002 | SWASP |
| 2454157.6459 | -4430.0 | 0.0165 | -4430.0 | -0.0027 | 0.0002 | SWASP |
| 2454158.4584 | -4428.0 | 0.0158 | -4428.0 | -0.0034 | 0.0001 | SWASP |
| 2454158.6624 | -4427.5 | 0.0165 | -4427.5 | -0.0027 | 0.0002 | SWASP |
| 2454159.4784 | -4425.5 | 0.0193 | -4425.5 | 0.0002 | 0.0001 | SWASP |
| 2454159.6790 | -4425.0 | 0.0166 | -4425.0 | -0.0025 | 0.0002 | SWASP |
| 2454160.4971 | -4423.0 | 0.0215 | -4423.0 | 0.0023 | 0.0001 | SWASP |
| 2454165.5854 | -4410.5 | 0.0273 | -4410.5 | 0.0081 | 0.0002 | SWASP |
| 2454166.5956 | -4408.0 | 0.0210 | -4408.0 | 0.0018 | 0.0002 | SWASP |
| 2454167.4047 | -4406.0 | 0.0169 | -4406.0 | -0.0022 | 0.0003 | SWASP |
| 2454167.6091 | -4405.5 | 0.0180 | -4405.5 | -0.0012 | 0.0002 | SWASP |
| 2454168.4249 | -4403.5 | 0.0206 | -4403.5 | 0.0014 | 0.0002 | SWASP |
| 2454169.4407 | -4401.0 | 0.0199 | -4401.0 | 0.0008 | 0.0002 | SWASP |
| 2454169.6348 | -4400.5 | 0.0107 | -4400.5 | -0.0084 | 0.0003 | SWASP |
| 2454170.4574 | -4398.5 | 0.0201 | -4398.5 | 0.0010 | 0.0002 | SWASP |
| 2454171.4745 | -4396.0 | 0.0207 | -4396.0 | 0.0016 | 0.0002 | SWASP |
| 2454194.4505 | -4339.5 | 0.0238 | -4339.5 | 0.0049 | 0.0002 | SWASP |
| 2454195.4645 | -4337.0 | 0.0213 | -4337.0 | 0.0024 | 0.0002 | SWASP |
| 2454204.4064 | -4315.0 | 0.0180 | -4315.0 | -0.0008 | 0.0002 | SWASP |
| 2454206.4388 | -4310.0 | 0.0174 | -4310.0 | -0.0014 | 0.0002 | SWASP |
| 2454208.4718 | -4305.0 | 0.0174 | -4305.0 | -0.0014 | 0.0002 | SWASP |
| 2454210.5040 | -4300.0 | 0.0166 | -4300.0 | -0.0022 | 0.0002 | SWASP |
| 2454219.4457 | -4278.0 | 0.0131 | -4278.0 | -0.0056 | 0.0002 | SWASP |
| 2455958.8674 | 0.0 | 0.0000 | 0.0 | -0.0059 | 0.0001 | Diethelm (2012) |
| 2455996.4842 | 92.5 | 0.0063 | 92.5 | 0.0007 | - | Hubscher et al. (2013) |
| 2456011.7308 | 130.0 | 0.0054 | 130.0 | -0.0001 | - | Diethelm (2012) |
| 2456014.5747 | 137.0 | 0.0031 | 137.0 | -0.0024 | - | Hubscher et al. (2013) |
| 2456740.3549 | 1922.0 | 0.0023 | 1922.0 | 0.0021 | - | Juryšek et al. (2017) |
| 2456744.6271 | 1932.5 | 0.0052 | 1932.5 | 0.0051 | - | Hubscher & Lehmann (2015) |

TABLE 1. CONTINUED

| HJD | $Epoch_{(1)}$ | $O\text{-}C_{(1)}$ | $Epoch_{(2)}$ | $O\text{-}C_{(2)}$ | Error | Source |
|---|---|---|---|---|---|---|
| 2456746.4543 | 1937.0 | 0.0027 | 1937.0 | 0.0026 | - | Juryšek et al. (2017) |
| 2458163.4530 | 5422.0 | 0.0004 | 5422.0 | 0.0107 | - | Lienhard (2018) |
| 2458240.7039 | 5612.0 | -0.0027 | 5612.0 | 0.0082 | - | This paper |

TABLE 2

TIMES OF MINIMA FOR CZEV188

| HJD | $Epoch_{(4)}$ | $O\text{-}C_{(4)}$ | Error | Source |
|---|---|---|---|---|
| 2457936.8949 | 7224.5 | -0.0009 | 0.0002 | This paper |
| 2458281.8967 | 8619.0 | 0.0007 | 0.0020 | This paper |

TABLE 3

TIMES OF MINIMA FOR CRTS J073333.0+302556

| HJD | $Epoch_{(5)}$ | $O\text{-}C_{(5)}$ | Error | Source |
|---|---|---|---|---|
| 2457771.8063 | 0.0 | -0.0006 | 0.0021 | This paper |
| 2457781.7049 | 37.0 | 0.0015 | 0.0015 | This paper |
| 2457787.8544 | 60.0 | -0.0009 | 0.0044 | This paper |

for several fixed values of the mass-ratio $q$ using as adjustable parameters the inclination of the systems $i$, the mean temperature of the secondaries $T_2$, the surface potentials $\Omega_1$=$\Omega_2$ for the contact systems, but $\Omega_1$ and $\Omega_2$ individually for the detached one, and the monochromatic luminosities of the primaries $L_1$. The behavior of the $q$-search for all the systems is shown in Figure 2.

The value of $q$ corresponding to the minimum of $\Sigma$ (the mean residuals for input data) was included in the list of the adjustable parameters and a more detailed analysis was performed simultaneously for all the available light curves for AF LMi and CzeV188 and separately for the light curves of CRTS J073333.0+302556. The amplitude of the light curve of CRTS J073333.0+302556 decreases with the increase of the wavelength: 0.44 mags in the $B$ filter, 0.30 in the $V$ filter and 0.22 in the $R$ filter, suggesting an increase in the contribution of the cooler (secondary) component to the system's total light (Zakirov & Shevchenko 1982). The strong wavelength dependency of the primary minima of CRTS J073333.0+302556 prevent us from dealing simultaneously with the light curves. Moreover, the light curves were treated with the Iglewicz and Hoaglin's test (Iglewicz & Hoaglin 1993) in order to exclude some deviating points.

For all the three systems, it was necessary to add a spot on the surface of one component to obtain a best fit of the data.

The WD code provides the "probable" errors of the adjustable parameters, which are derived by the differential correction routine. It is known that they are unrealistically small. With the purpose of obtaining an independent estimate of the uncertainties of these parameters, we approached the problem through the Markov Chain Monte Carlo (MCMC) procedure. We generated many different data samples of the free parameters; the correlations among them from MCMC simulations and histograms of individual parameter distributions for AF LMi, CzeV188 and CRTS J073333.0+302556 are shown in Figures. 3 - 5.

The final light curve solutions, with the uncertainties derived from the MCMC procedure are reported in Tables 4 and 5, while in Figure 6 we present the filtered solution curves overlaying the data and the geometrical surface representations of the systems respectively.

TABLE 4

LIGHT CURVES SOLUTION FOR AF LMI AND CZEV188

| | AF LMi | Error | CzeV188 | Error |
|---|---|---|---|---|
| $i$ (°) | 76.085 | 0.578 | 73.879 | 0.578 |
| $T_1$ (K) | 5700 | fixed | 5270 | fixed |
| $T_2$ (K) | 5379 | 57 | 5152 | 86 |
| $\Omega_1 = \Omega_2$ | 8.103 | 0.287 | 8.763 | 0.116 |
| $q$ | 4.300 | 0.115 | 4.760 | 0.087 |
| $f$ | 0.296 | 0.012 | 0.162 | 0.009 |
| $L_{1B}$ | 0.263 | 0.020 | 0.210 | 0.009 |
| $L_{2B}$ | 0.677 | 0.013 | 0.734 | 0.001 |
| $L_{1V}$ | 0.249 | 0.011 | 0.206 | 0.006 |
| $L_{2V}$ | 0.685 | 0.012 | 0.743 | 0.001 |
| $L_{1R}$ | 0.242 | 0.012 | 0.203 | 0.003 |
| $L_{2R}$ | 0.700 | 0.008 | 0.747 | 0.001 |
| $L_{1I}$ | 0.243 | 0.010 | 0.201 | 0.001 |
| $L_{2I}$ | 0.705 | 0.007 | 0.753 | 0.001 |
| Primary | | | | |
| $r$ (pole) | 0.2540 | 0.0007 | 0.2418 | 0.0007 |
| $r$ (side) | 0.2658 | 0.0008 | 0.2523 | 0.0008 |
| $r$ (back) | 0.3087 | 0.0017 | 0.2899 | 0.0016 |
| Secondary | | | | |
| $r$ (pole) | 0.4856 | 0.0004 | 0.4887 | 0.0004 |
| $r$ (side) | 0.5289 | 0.0005 | 0.5235 | 0.0006 |
| $r$ (back) | 0.5557 | 0.0007 | 0.5570 | 0.0008 |
| lat spot (°) | 74.21 | 1.5 | 79.58 | 1.7 |
| long spot (°) | 226.43 | 1.1 | 301.33 | 0.8 |
| Radius (°) | 17.56 | 0.5 | 30.15 | 0.7 |
| Temp. Fact. | 0.91 | 0.06 | 0.97 | 0.03 |
| Star | 2 | | 1 | |
| $\Sigma$ | 0.001795 | | 0.000769 | |

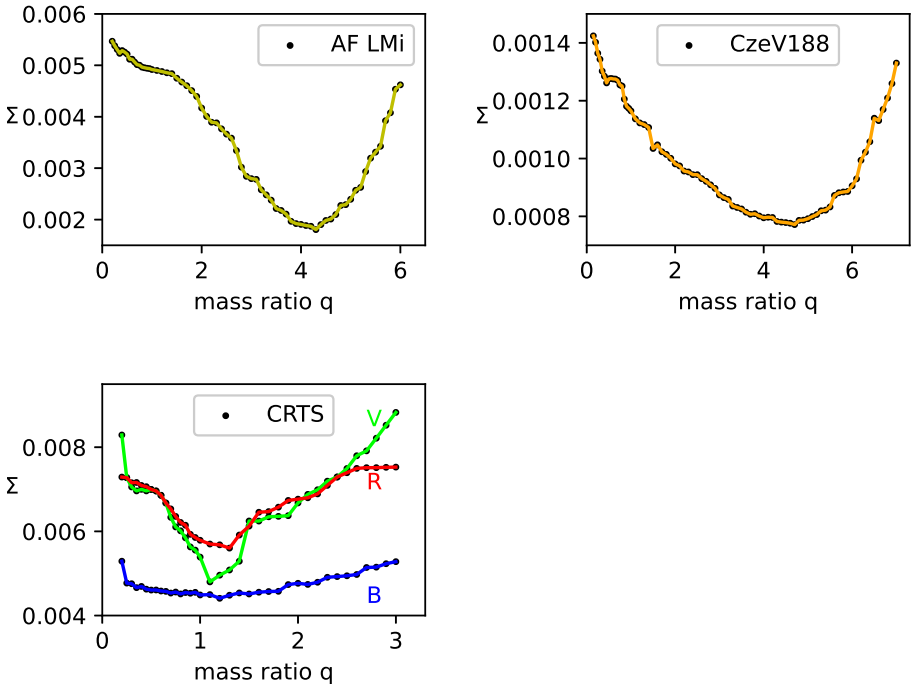


Fig. 2. The relation Σ (the mean residuals for input data) versus mass-ratio $q$. The color figure can be viewed online.

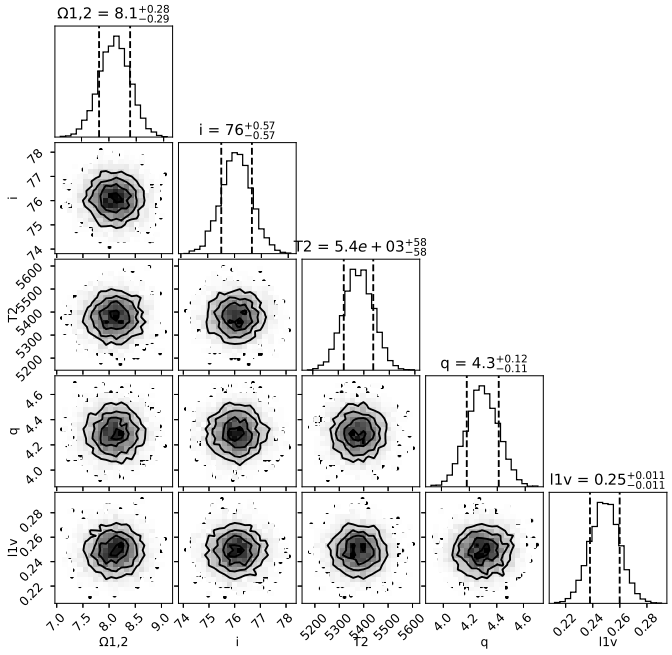


Fig. 3. Parameter correlations resulting from MCMC fit and histograms of individual parameter distributions for AF LMi.

## 5. ESTIMATION OF THE PHYSICAL PARAMETERS OF AF LMI AND CZEV188 WITH THE GAIA PARALLAX

Physical parameters such as mass, radius and luminosity are very important information for a contact binary system. Here we will introduce how we have estimated the physical parameters of AF LMi and CzeV188, without knowing their radial velocity curves, by using the parallaxes reported by Gaia (Gaia Collaboration et al. 2018). First, we

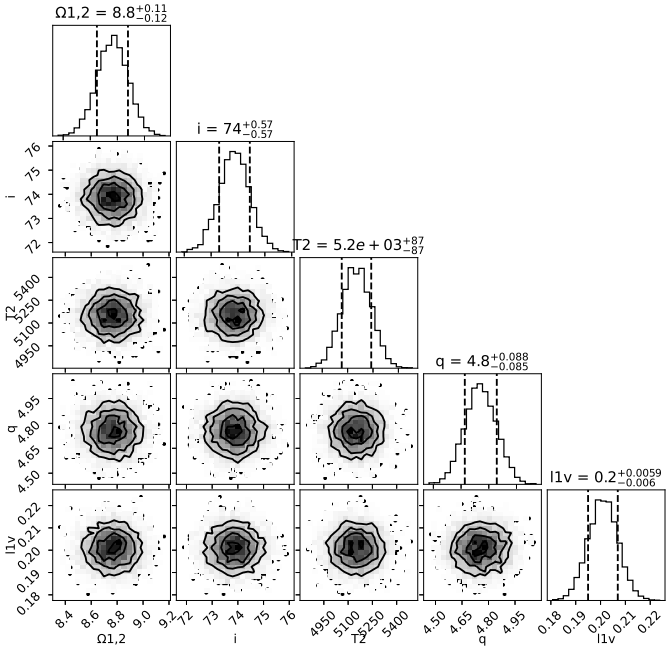


Fig. 4. The same of Figure 3 but for CzeV188.

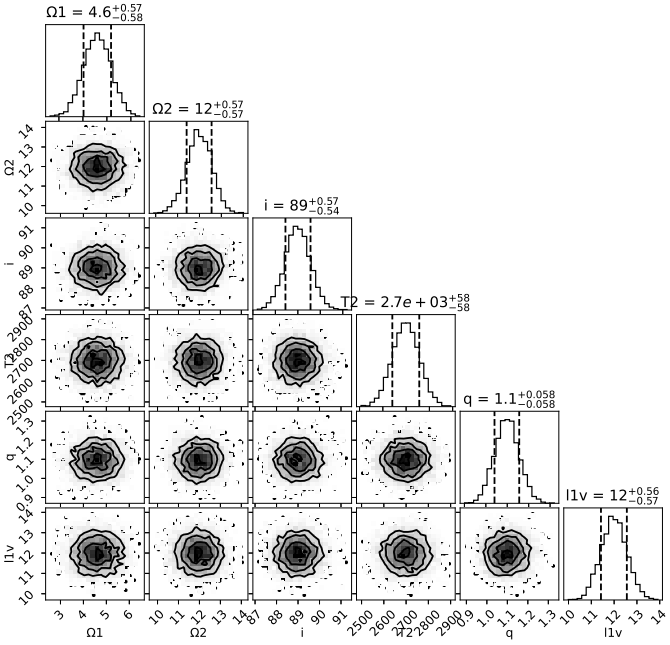


Fig. 5. The same of Figure 3 but for CRTS J073333.0+302556 in V Filter.

calculated the Galactic extinction using two different methods: for AF LMi ($A_v = 0.1892$) the spiral model from Amôres & Lépine (2005) using the code GALEextin.[8] For CzeV188 ($A_v = 0.7285$) we used the methodology of Arenou et al. (1992) since its galactic latitude is between -5° < b < +5°.

[8] http://www.galextin.org/interstellar_extinction.php.

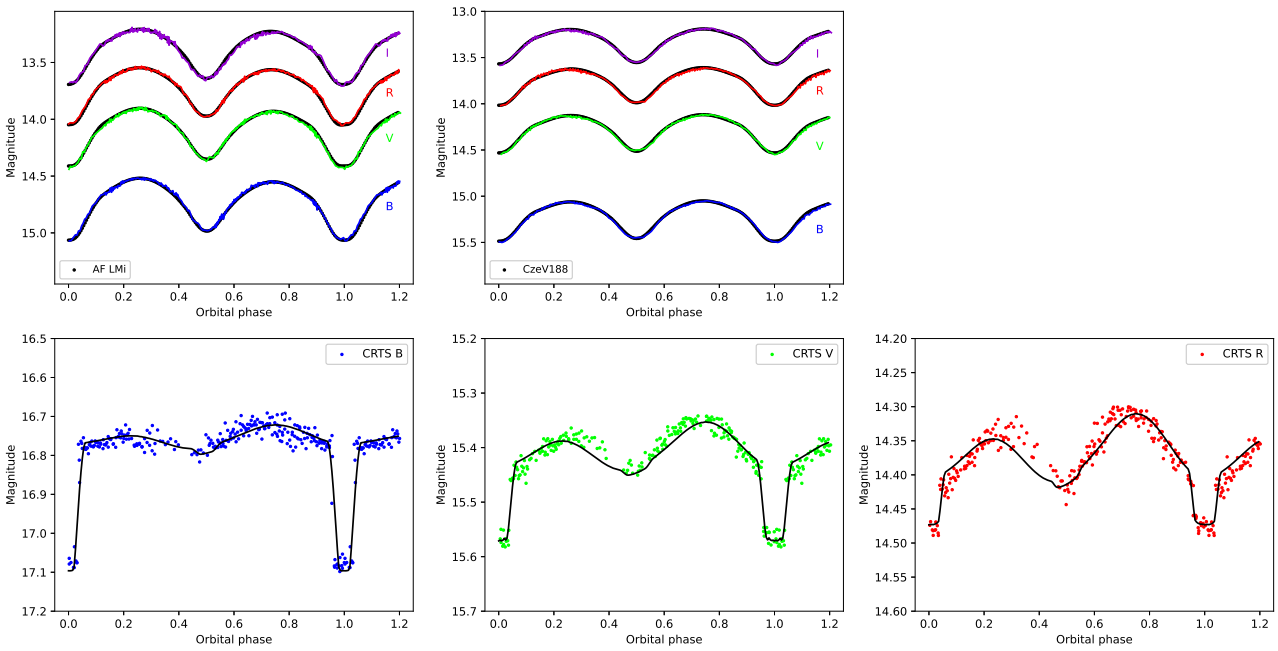


Fig. 6. CCD light curves for the three systems. Points are the original observations, color lines are the theoretical light curves. The color figure can be viewed online.



Knowing the parallax from Gaia, AF LMi p[mas] 0.986±0.017 and distance $d_{pc}$ 1014.2±0.017, CzeV188 p[mas] 2.260±0.013 and $d_{pc}$ 442.46±3.60, we calculated the visual absolute magnitude $M_v$, the bolometric magnitude $M_{bol}$, the total luminosity $L_{tot}$ and the individual luminosities $L_{1,2}$ with the following equations (e.g. Chen et al. 2018):

$$M_v = m_v - 5\log(1000/\pi) + 5 - A_v\,, \tag{6}$$

where $m_v$ is the dereddened $V$ magnitude.

$$M_{bol} = M_v + BC\,. \tag{7}$$

Here $BC$ is the star's bolometric correction as interpolated from the Pecaut & Mamajek (2013) tables.

$$\log(L_{tot}/L_\odot) = 0.4(4.74 - M_{bol})\,, \tag{8}$$

$$L_1 = L_{tot}/(c)\,, \tag{9}$$

where $c = \mathrm{L_{2V}/L_{1V}}$, see Table 4

$$L_2 = L_{tot} - L_1\,. \tag{10}$$

The temperatures of the first and second component of the system are known, so we obtained their radii $\mathrm{R_{1,2}}$, the semiaxis, $a$, and the total mass of the systems from Kepler's third law.

$$R_{1,2}[R_\odot] = L_{1,2}^{(1/2)}/(T_{1,2}/[T_\odot])^2\,, \tag{11}$$

where $[T_\odot] = 5771.8$K.

$$a = R_1/r_{1mean}$$

$$M_{tot} = 0.0134(a^3/P^2)\,, \tag{12}$$

where $P$ is the period in days.

Using the value of the mass ratio from the Wilson-Devinney analysis, finally we obtained the masses $M_1$ and $M_2$. The values of all parameters are shown in Table 6.

## 6. ESTIMATION OF THE ABSOLUTE ELEMENTS OF CRTS J073333.0+302556

Due to the lack of radial velocity (RV) solutions, we used empirical relations to determine the absolute parameters of the binary systems. Dimitrov & Kjurkchieva (2015) gave a period - semi-major axis ($P$,$a$) relation on the basis of 14 binary stars having $P < 0.27$d which had both RV and photometric solutions, which is approximated by a parabola:

$$a = -1.154 + 14.633 \times P - 10.319 \times P^2,$$

where $P$ is in days and $a$ is in solar radii.

Using the semi-major axis, we can calculate the radii of the binary components as $R_{1,2} = a \times r_{1,2}$ mean, where $r_{1,2}$ mean is the mean fractional radii of the components. Considering a solar temperature of

TABLE 5

LIGHT CURVES SOLUTION FOR CRTS J073333.0+302556

| | $B$ Filter | Error | $V$ Filter | Error | $R$ Filter | Error |
|---|---|---|---|---|---|---|
| $i$ (°) | 89.204 | 0.478 | 89.384 | 0.577 | 89.527 | 0.848 |
| $T_1$ (K) | 4027 | fixed | 4027 | fixed | 4027 | fixed |
| $T_2$ (K) | 2903 | 19 | 2748 | 57 | 2760 | 8 |
| $\Omega_1$ | 5.394 | 0.176 | 4.602 | 0.577 | 4.827 | 0.105 |
| $\Omega_2$ | 10.697 | 1.118 | 12.004 | 0.577 | 19.077 | 0.506 |
| $q$ | 1.2068 | 0.0068 | 1.0863 | 0.0577 | 1.2961 | 0.0026 |
| $f_1$ | -0.246 | 0.007 | -0.146 | 0.004 | -0.117 | 0.008 |
| $f_2$ | -0.600 | 0.009 | -0.660 | 0.010 | -0.764 | 0.006 |
| $L_{1B}$ | 12.177 | 0.006 | | | | |
| $L_{2B}$ | 0.139 | 0.003 | | | | |
| $L_{1V}$ | | | 12.079 | 0.573 | | |
| $L_{2V}$ | | | 0.071 | 0.002 | | |
| $L_{1R}$ | | | | | 12.167 | 0.008 |
| $L_{2R}$ | | | | | 0.071 | 0.003 |
| Primary | | | | | | |
| $r$ (pole) | 0.2354 | 0.0117 | 0.2818 | 0.0085 | 0.2795 | 0.0088 |
| $r$ (side) | 0.2390 | 0.0125 | 0.2887 | 0.0095 | 0.2869 | 0.0098 |
| $r$ (back) | 0.2445 | 0.0140 | 0.2994 | 0.0112 | 0.2996 | 0.0119 |
| Secondary | | | | | | |
| $r$ (pole) | 0.1223 | 0.0140 | 0.0982 | 0.0050 | 0.0711 | 0.0020 |
| $r$ (side) | 0.1225 | 0.0141 | 0.0983 | 0.0051 | 0.0711 | 0.0020 |
| $r$ (back) | 0.1228 | 0.0142 | 0.0984 | 0.0051 | 0.0712 | 0.0020 |
| lat spot (°) | 90 | fixed | 90 | fixed | 90 | fixed |
| long spot (°) | 250.56 | 1.9 | 250.34 | 2.1 | 250.78 | 1.7 |
| Radius (°) | 25.68 | 1.3 | 25.44 | 0.9 | 25.12 | 1.3 |
| Temp. Fact. | 0.98 | 0.04 | 0.97 | 0.03 | 0.97 | 0.06 |
| Star | 1 | | 1 | | 1 | |



$T_\odot = 5771.8$ K, the luminosities can be calculated using the equation: $L_{1,2} = (R_{1,2}/R_\odot)^2 \times (T_{1,2}/T_\odot)^4$. The mean densities of the binary components were derived from the following equation given by Mochnacki (1981): $\rho_1 = 0.0189/[r^3_{1mean}P^2(1+q)]$ and $\rho_2 = 0.0189q/[r^3_{2mean}P^2(1+q)]$.

All the above calculated values are listed in Table 7.

The results here presented for CRTS J073333.0+302556 are a preliminary solution.

## 7. DISCUSSION ON THE SYSTEMS

Here we have presented the analysis of filtered CCD light curves of two contact binary systems. For both we calculated the orbital angular momentum $J_0$ (Eker et al. 2006) and their position in the $\log J_0 - \log M$ diagram. With a value of $\log J_0$ as reported in Table 6, the systems are beyond the curved limit separating the detached and contact systems, in the region of the contact stars, which supports the shallow-contact geometric situation (Figure 8). From Figure 1, the trend of O-C (solid line) shows parabolic compositions with a rate of $dP/dt = 3.61 \times 10^{-7} \pm 7.41^{-8}$ days year$^{-1}$. This long-term increase can probably be explained by the mass transfer from the less massive star to the more massive star. Then, if we assume conservative mass transfer, the following equation can be used to calculate the mass transfer between the components of AF LMi:

$$\dot{P}/P = -3\dot{M}_1(1/M_1 - 1/M_2). \quad (13)$$

Combining the parameters (including mass, period and rate of period variation) the rate of mass transfer was determined as

$$dM_1/dt = -1.97 \times 10^{-7} M_\odot \text{ years}^{-1}.$$

TABLE 6

ESTIMATED ABSOLUTE ELEMENTS FOR AF LMI AND CZEV188

| Target | $L_1(L_\odot)$ | $L_2(L_\odot)$ | $R_1(R_\odot)$ | $R_2(R_\odot)$ | $a$ $(R_\odot)$ | $M_1(M_\odot)$ | $M_2(M_\odot)$ |
|---|---|---|---|---|---|---|---|
| AF LMi | $0.752 \pm 0.029$ | $2.064 \pm 0.120$ | $0.889 \pm 0.017$ | $1.654 \pm 0.054$ | $3.219 \pm 0.074$ | $0.510 \pm 0.170$ | $2.193 \pm 0.060$ |
| CzeV188 | $0.267 \pm 0.009$ | $0.960 \pm 0.034$ | $0.620 \pm 0.011$ | $1.230 \pm 0.022$ | $2.372 \pm 0.042$ | $0.507 \pm 0.026$ | $2.413 \pm 0.012$ |
| | $J$ | $\log J$ | $J_{lim}$ | $\log J_{lim}$ | Sp. type | $\log \rho_1(gr/cm^3)$ | $\log \rho_2(gr/cm^3)$ |
| AF LMi | $7.38^{51}$ | 51.87 | 52.14 | $1.37^{52}$ | G3 + G9 | 0.01 | -0.19 |
| CzeV188 | $6.66^{51}$ | 51.82 | 52.12 | $1.62^{52}$ | K0 + K1 | 0.48 | 0.25 |

*Note*: Spectral types are according to Pecaut & Mamajek (2013).

TABLE 7

ESTIMATED ABSOLUTE ELEMENTS FOR CRTS J073333.0+302556 (V FILTER)

| $L_1(L_\odot)$ | $L_2(L_\odot)$ | $R_1(R_\odot)$ | $R_2(R_\odot)$ | $a$ $(R_\odot)$ | $M_1(M_\odot)$ | $M_2(M_\odot)$ |
|---|---|---|---|---|---|---|
| $0.084 \pm 0.003$ | $0.002 \pm 0.001$ | $0.595 \pm 0.011$ | $0.199 \pm 0.073$ | $2.022 \pm 0.001$ | $0.742 \pm 0.002$ | $0.891 \pm 0.005$ |
| $J$ | $\log J$ | $J_{lim}$ | $\log J_{lim}$ | Sp. type | $\log \rho_1(gr/cm^3)$ | $\log \rho_2(gr/cm^3)$ |
| $4.13^{51}$ | 51.62 | 55.21 | $1.63^{55}$ | K8 + M6 | 0.70 | 2.16 |

*Note*: Spectral types are according to Pecaut & Mamajek (2013).



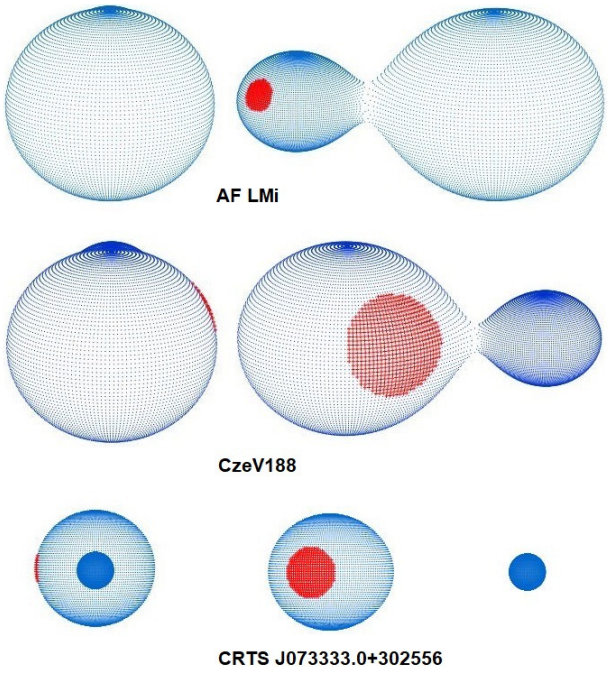


Fig. 7. The 3D view of the stars. Left at the primary minimum, right at the quadrature. The color figure can be viewed online.

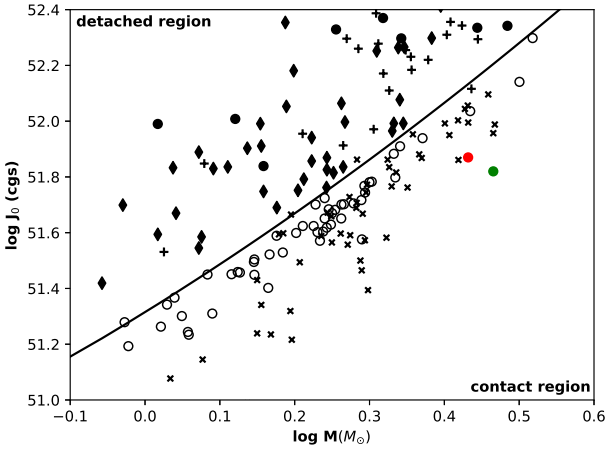


Fig. 8. Position of AF LMi (red dot) and CzeV188 (green dot) in the $\log J_0 - \log M$ diagram. As explained in Figure 1 of the original paper of Eker et al. (2006) symbols mean: Giants (•), Sub-Giants (+), Main-Sequence (⧫), A-subtype (×), W-subtype (○). The color figure can be viewed online.

The negative sign indicates that the less massive component $M_1$ is losing mass, while the more massive component $M_2$ is gaining mass. As the mass ratio increases, so does the separation between the two components. The degree of contact would decrease, and AF LMi will evolve from the present contact state to the semi-contact or detached binary state.

Because the sums of the mean fractional radii of the components are $r_{mean} = 0.799$ and $r_{mean} = 0.784$, for AF LMi and CzeV188 respectively, they are in a state of marginal contact (Kopal, 1959).

### 7.1. *AF LMi and CzeV188*

The values of mass ratio found for AF LMi and CzeV188 indicate that they are typical W-subtype

contact binaries. A-and W-subtype are two groups of the W UMa systems divided in these subclasses by Binnendijk(1965, 1970). In the A-subtype systems the larger star is the hottest and the primary eclipse is a transit. In W-type the opposite is true: the smaller star is the hottest and the primary eclipse is an occultation. Both types of systems have a shallow fill-out value and a small difference in temperature between the components, i.e good thermal contact, these characteristics are generally accepted for over-contact systems. The O'Connell effect (O'Connell 1951) that explains the different heights of the maxima, is visible; a cool spot on the secondary component of AF LMi and a cool spot on the primary component of CzeV188 (inverse O'Connell effect) were added to obtain the best fit to the light curves. The cool spot, in contrast to the hot spot, is connected with magnetic activity of the same nature as solar magnetic spots (Mullan 1975); the hot spot is generally due to the impact of the mass transferred between the components (Lee et al. 2006). CzeV188, with its short orbital period (<0.3 days) and its spectral type K, suggests that it is near the shortest period limit. Following the work of Qian et al. (2020), who investigated in detail the period-temperature relation using the LAMOST stellar atmospheric parameters and constructed the heat map for this relation as shown in our Figure 9 (Figure 4 in the original paper), it is possible to see that AF LMi (red dot) and CzeV188 (green dot) in this graph are located inside the boundaries for normal EW systems, but with different positions. In fact, the red and blue lines are the boundaries of the normal EW systems. Near the red line are found marginal contact systems, while those close to the blue line are deep contact ones. The objects between the two lines are normal contact EW systems.

AF LMi, with its fill-out factor and the difference in temperature between its component of some hundreds of K, is located near the red border, indicating that it could be either at the end or at the beginning of the contact phase, as predicted by the TRO theory. CzeV188 shows good thermal contact since the difference in temperature between the components is less than 100K. It is located far from the red border and near the blue one. This suggests that it is approaching the final stage of contact binary evolution.

### 7.2. *CRTS J073333.0+302556*

CRTS J073333.0+302556 is a rare M dwarf detached system with non-degenerate components. As discussed in Becker et al. (2011), the sample of known binary systems composed of two dwarfs is

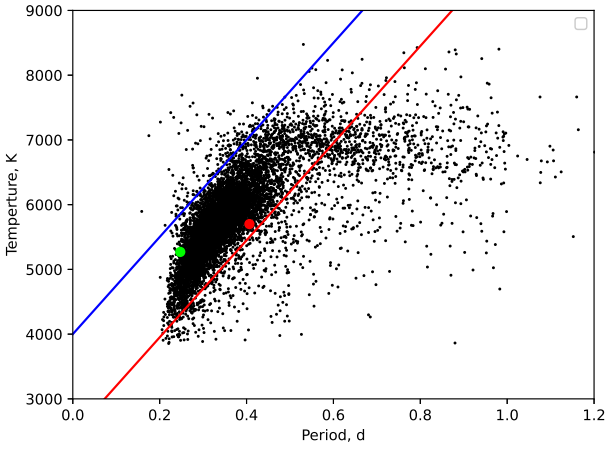


Fig. 9. Correlation between orbital period and temperature based on parameters of 8510 contact binaries from Qian et al. (2020). The position of AF LMi is marked in red, the one of CzeV188 in green. The red and blue lines are the boundaries of normal EWs. The color figure can be viewed online.

very small. Its light curve shows a strong wavelength dependency at the primary minima. The amplitude of the light curve decreases with increasing wavelength; this suggest an increase in the contribution of the cooler (secondary) component to the system's total light (Zakirov & Shevchenko 1982). Also visible is the shallower secondary eclipse, which becomes deeper in the redder bands. In addition it is seen that there is a small difference in the height of the maxima with the secondary higher than the primary, so it was necessary to add a cool spot on the surface of the first component in order to account for this characteristic.

A graphical representation and the Roche geometry of CRTS J073333.0+302556 is depicted in Figure 7.

This work has made use of data from the European Space Agency (ESA) mission Gaia, [9] and processed by the Gaia Data Processing and Analysis Consortium (DPAC).[10]

Use of the International Variable Star Index (VSX) database has been made (operated at AAVSO Cambridge, Massachusetts, USA), as well as of the AAVSO Photometric All-Sky Survey (APASS) funded by the Robert Martin Ayers Sciences Fund. Also, use has been made of the VizieR catalogue access tool, CDS, Strasbourg, France. The original

[9] https://www.cosmos.esa.int/gaia.
[10] https://www.cosmos.esa.int/web/gaia/dpac/consortium.

description of the VizieR service was published in A&AS 143, 23.

Based upon observations carried out at the Observatorio Astronómico Nacional on the Sierra San Pedro Mártir (OAN-SPM), Baja California, México.

We would like to thank the anonymous referee for all her/his very useful comments and corrections which have improved the quality of this paper.

## REFERENCES

Amôres, E. B. & Lépine, J. R. D. 2005, AJ, 130, 659, https://doi.org/10.1086/430957

Arenou, F., Grenon, M., & Gomez, A. 1992, A&Ap, 258, 104

Bai, Y., Liu, J., Bai, Z., Wang, S., & Fan, D. 2019, AJ, 158, 93

Becker, A. C., Bochanski, J. J., Hawley, S. L., et al. 2011, ApJ, 731, 17, https://doi.org/10.1088/0004-637X/731/1/17

Binnendijk, L. 1965, VeBam, 27, 36

_____. 1970, VA, 12, 217, https://doi.org/10.1016/0083-6656(70)90041-3

Butters, O. W., West, R. G., Anderson, D. R., et al. 2010, A&Ap, 520, 10, https://doi.org/10.1051/0004-6361/201015655

Chen, X., Deng, L., de Grijs, R., Wang, S., & Feng, Y. 2018, ApJ, 859, 140, https://doi.org/10.3847/1538-4357/aabe83

Claret, A. & Bloemen, S. 2011, A&Ap, 529, 75, https://doi.org/10.1051/0004-6361/201116451

Diethelm, R. 2012, IBVS, 6029, 1

Dimitrov, D. P. & Kjurkchieva, D. P. 2015, MNRAS, 448, 2890, https://doi.org/10.1093/mnras/stv147

Drake, A. J., Graham, M. J., Djorgovski, S. G., et al. 2014, ApJS, 213, 9, https://doi.org/10.1088/0067-0049/213/1/9

Eker, Z., Demircan, O., Bilir, S., & Karataş, Y. 2006, MNRAS, 373, 1483, https://doi.org/10.1111/j.1365-2966.2006.11073.x

Flannery, B. P. 1976, ApJ, 205, 217, https://doi.org/10.1086/154266

Fukugita, M., Ichikawa, T., Gunn, J. E., et al. 1996, AJ, 111, 1748, https://doi.org/10.1086/117915

Gaia Collaboration, Brown, A. G. A., Vallenari, A., et al. 2018, A&Ap, 616, 1, https://doi.org/10.1051/0004-6361/201833051

Hubscher, J., Braune, W., & Lehmann, P. B. 2013, IBVS, 6048, 1

Hubscher, J. & Lehmann, P. B. 2015, IBVS, 6149, 1

Juryšek, J., Hoňková, K., Šmelcer, L., et al. 2017, OEJV, 179, 1

Kochanek, C. S., Shappee, B. J., Stanek, K. Z., et al. 2017, PASP, 129, 104502, https://doi.org/10.1088/1538-3873/aa80d9

Kopal, Z. 1959, Close Binary Systems, The International Astrophysics Series (London: Chapman & Hall)

Khruslov, A. V. 2007, PZP, 7, 6

Iglewicz, B., & Hoaglin, D., 1993, The ASQC Basic References in Quality Control: Statistical Techniques in How to Detect and Handle Outliers, ed. E. F. Mykytka (Milwaukee, WI: ASQC Quality Press)

Gaia Collaboration. 2018, VizieR Online Data Catalog, I/345

Landolt, A. U. 2009, AJ, 137, 4186, https://doi.org/10.1088/0004-6256/137/5/4186

Lee, J.-W., Lee, C.-U., Kim, C.-H., & Kang, Y.,-W. 2006, JKAS, 39, 41, https://doi.org/10.5303/JKAS.2006.39.2.041

Li, L., Zhang, F., Han, Z., Jiang, D., & Jiang, D. 2008, MNRAS, 387, 97, https://doi.org/10.1111/j.1365-2966.2008.12736.x

Lienhard, P. 2008, BAV Journal, 31, 19

Liu, N.-P., Qian, S.-B., Soonthornthum, B., et al. 2014, AJ, 147, 41, https://doi.org/10.1088/0004-6256/147/2/41

Lucy, L. B. 1976, ApJ, 205, 208, https://doi.org/10.1086/154265

Luo, A.-L., Zhao, Y.-H., Zhao, G., et al. 2016, VizieR Online Data Catalog, V/149

_____. 2019, VizieR Online Data Catalog, V/164

Marsh, F. M., Prince, T. A., Mahabal, A. A., et al. 2017, MNRAS, 465, 4678, https://doi.org/10.1093/mnras/stw2110

Milano, L. & Russo, G. 1983, MNRAS, 203, 235, https://doi.org/10.1093/mnras/203.2.235

Mochnacki, S. W. 1981, ApJ, 245, 650, https://doi.org/10.1086/158841

Mullan, D. J. 1975, ApJ, 198, 563, https://doi.org/10.1086/153635

O'Connell, D. J. K. 1951, Publications of the Riverview College Observatory, 2, 85

Pecaut, M. J. & Mamajek, E. E. 2013, ApJS, 208, 9, https://doi.org/10.1088/0067-0049/208/1/9

Qian, S.-B., Zhu, L.-Y., Liu, L., et al. 2020, RAA, 20, 163, https://doi.org/10.1088/1674-4527/20/10/163

Robertson, J. A. & Eggleton, P. P. 1977, MNRAS, 179, 359, https://doi.org/10.1093/mnras/179.3.359

Shappee, B. J., Prieto, J. L., Grupe, D., et al. 2014, ApJ, 788, 48, https://doi.org/10.1088/0004-637X/788/1/48

Skarka, M., Mašek, M., Brát, L., et al. 2017, OEJV, 185, 1

Svechnikov, M. A. & Taidakova, T. A. 1984, SvA, 28, 84

Tonry, J. L., Denneau, L., Flewelling, H., et al. 2018, ApJ, 867, 105, https://doi.org/10.3847/1538-4357/aae386

van Hamme, W. 1993, AJ, 106, 2096, https://doi.org/10.1086/116788

Wilson, R. E. & Devinney, E. J. 1971, ApJ, 166, 605, https://doi.org/10.1086/150986

Wilson, R. E. 1990, ApJ, 356, 613, https://doi.org/10.1086/168867

_____. 1994, PASP, 106, 921, https://doi.org/10.1086/133464

Wilson, R. E. & van Hamme, W. 2016, Computing Binary Stars Observables. <ftp.astro.ufl.edu>, directory pub/wilson/lcdc2015

Worthey, G. & Lee, H.-ch. 2011, ApJS, 193, 1, https://doi.org/10.1088/0067-0049/193/1/1

Yakut, K. & Eggleton, P. P. 2005, ApJ, 629, 1055, https://doi.org/10.1086/431300

Zakirov, M. M. & Shevchenko, V. S. 1982, PZ, 21, 629



F. Acerbi: Via Zoncada 51, Codogno, LO, 26845, Italy (acerbifr@tin.it).

L. Altamirano-Dévora: Carretera Tijuana-Ensenada 3917, 22860 Ensenada, BC, Mexico (altamirano.l18@gmail.com).

C. Barani: Via Molinetto 35, Triulza di Codogno, LO, 26845, Italy (cvbarani@alice.it).

M. Martignoni: Via Don G. Minzoni 26/D, Magnago, MI, 20020, Italy (massimiliano.martignoni@outlook.it).

R. Michel: Instituto de Astronomia, UNAM. A.P. 877, 22800 Ensenada, BC, Mexico (rmm@astro.unam.mx).